M-2341

J. Chem. Thermodynamics **1989**, 21, 363–373

FeAs: Heat capacity, enthalpy increments, other thermodynamic properties from 5 to 1350 K, and magnetic transition[a]

DOMINGO GONZALEZ-ALVAREZ,

Facultad de Ciencias de la Universidad de Zaragoza, Departamento de Fisica Fundamental, 5009 Zaragoza, Spain

FREDRIK GRØNVOLD,

Chemical Institute, University of Oslo, Blindern, Oslo 3, Norway

BENGT FALK,[b] EDGAR F. WESTRUM, JR.,

Department of Chemistry, University of Michigan, Ann Arbor, MI 48109, U.S.A.

R. BLACHNIK,[c] and G. KUDERMANN[d]

Technical University, Siegen, Federal Republic of Germany

(Received 2 January 1989)

The heat capacity of iron monoarsenide has been determined by adiabatic calorimetry from 5 to 1030 K and by drop calorimetry relative to 298.15 K over the range 875 to 1350 K. A small λ-type transition is observed at $T_N = (70.95 \pm 0.02)$ K. It is related to the disappearance of a doubly helically ordered magnetic-spin structure on heating. The obviously cooperative entropy increment of transition is only $\Delta_{trs}S^\circ_m/R = 0.021$. The higher-temperature heat capacity rises considerably above lattice expectations. Part of the rise is ascribed to low-spin electron redistribution in iron, while the further excess above 800 K presumably arises from a beginning low- to high-spin transition, possibly connected with interstitial defect formation in the MnP-type structure. FeAs melts at about 1325 K with $\Delta_{fus}H^\circ_m = 6180R \cdot$ K. Thermodynamic functions have been evaluated and the values of $C_{p,m}(T)$, $S^\circ_m(T)$, $H^\circ_m(T)$, and $\Phi^\circ_m(T)$, are $6.057R$, $7.513R$, $1177R \cdot$ K, and $3.567R$ at 298.15 K, and $8.75R$, $16.03R$, $6287R \cdot$ K, and $9.745R$ at 1000 K.

[a] The low-temperature measurements completed at the University of Michigan were supported in part by the Structural Chemistry and Chemical Thermodynamics Program, Division of Chemistry, National Science Foundation under grant CHE-8007977.

[b] Present address: Alfastar AB, S-223 70 Lund, Sweden.

[c] Present address: F. B. Biologie Chemie, Universität Osnabrück, Postfach D 4500, Osnabrück, F.R.G.

[d] Present address: Leichtmetall-Forschungsinstitut der VAW Vereinigte Aluminium-Werke AG, D-5300 Bonn 1, Postfach 2468, F.R.G.

0021-9614/89/040363+11 $02.00/0

1. Introduction

Iron monoarsenide with the MnP-type crystal structure shows an interesting magnetic helical structure which disappears at 77 K.[1] The fact that all known examples of magnetically ordered MnP-type structures belong to the helimagnetic class—except the prototype which is ferromagnetic over the interval $50\ \text{K} < T < 291\ \text{K}$—strongly suggests that this pattern is a consequence of the metal-atom sublattice arrangement. The associated energetic changes have not yet been determined. One purpose of this study was to provide thermodynamic quantities about the compound and its magnetic transition as we have done for the related compound CrAs.[2] Another was to determine the enthalpy of fusion of FeAs with our drop calorimeter.

The structure of FeAs was first studied by Hägg,[3-5] who found that it was orthorhombic and related to that of NiAs. FeAs was later shown to be isostructural with MnP.[6,7] The NiAs-type regular trigonal antiprismatic coordination of non-metal atoms around each metal atom is distorted in the MnP-type (Pnam) with four sets of different metal-to-non-metal bond lengths (2+2+1+1). It was later thought[8] that the space group $Pna2_1$ was applicable to FeAs. This space group lacks a mirror plane compared with space group Pnam, and thus none of the six Fe–As bond lengths would be equal by symmetry. In view of the insignificant deviation of y_{As} from 1/4 in $Pna2_1$, it was later concluded that the correct space group is Pnam.[9,10] Lyman and Prewitt[11] also concluded that the insignificant changes in interatomic distances between the two models support the choice of Pnma.

The X-ray and neutron-diffraction studies show[1,8,9] that the FeAs is closely stoichiometric and that the MnP-type structure persists essentially unchanged between 12 and about 1325 K. Below 77 K the iron atoms order in a double spiral arrangement, with helical axis along *b*, and with pitch incommensurate with the cell length. The value of the magnetic moment indicates low-spin conditions in the cooperative state. The increasing magnetic susceptibility up to a maximum at 250 K, the Curie–Weiss behavior in the range 300 to 800 K, and the slight increase above 850 K, indicate changing population of excited 3d-electron states or narrow bands. These changes should be noticeable also in the higher-temperature heat capacity.

2. Experimental

The sample was synthesized at Clausthal from the elements. Iron of 99.97 mass per cent purity was donated by the Max Planck Institute in Düsseldorf, while the 99.9999 mass per cent crystalline arsenic was obtained from Preussag, F.R.G. Stoichiometric mixtures of the elements (70 to 100 g) were heated in evacuated and sealed vitreous-silica ampoules at 920 K for 2 d and then up to 1170 K over a period of 5 d. The products were crushed finely and tempered at 1120 K for 10 d. The crushing and heating procedure was repeated in order to ascertain homogeneity of the sample. The sample was examined by X-ray powder diffraction, using a Guinier camera of 80 mm diameter, Cu $K\alpha_1$ radiation, and KCl {a(298.15 K) =

629.19 pm}[12] as a calibrating substance. The orthorhombic lattice constants are $a = 544.3 \pm 0.1$, $b = 337.4 \pm 0.1$, $c = 602.8 \pm 0.1$ pm; in good agreement with the results by Selte and Kjekshus:[8] $a = 544.20 \pm 0.7$, $b = 337.27 \pm 0.6$, $c = 602.78 \pm 0.7$ pm, and with those of Lyman and Prewitt:[11] $a = 544.0 \pm 0.5$, $b = 337.12 \pm 0.04$, $c = 602.59 \pm 0.05$ pm.

CALORIMETRIC TECHNIQUE

5 *to* 350 K, *University of Michigan.* The heat capacity of FeAs was measured in the Mark-II adiabatic calorimetric cryostat described elsewhere.[13] A gold-plated copper calorimeter (W-52) with a volume of 59 cm^3 was used. Temperatures were measured with a capsule-type platinum-resistance thermometer (A-5) located in a central well in the calorimeter. The calorimeter was loaded with sample, evacuated, and helium gas added at 7.2 kPa pressure to provide thermal contact between sample and calorimeter. It was then sealed, placed in the cryostat, and cooled. The platinum resistance thermometer had been calibrated by the U.S. National Bureau of Standards (NBS). Temperatures are judged to correspond to IPTS-68 within 0.02 to 350 K. Measurements of mass, resistance, potential, and time are referred to standardizations and calibrations performed at NBS.

The heat capacity of the empty calorimeter was determined in a separate series of experiments. The heat capacity of the 151.51 g sample represented from 70 to 80 per cent of the total. Small corrections were applied for temperature excursions of the shields from the calorimeter temperature and for "zero drift" of the calorimeter temperature. Further, small corrections were applied for differences in masses of the sealing gold gasket and helium gas between the loaded and empty calorimeter.

300 *to* 1030 K, *University of Oslo.* The calorimetric apparatus and measuring technique have been described.[14] The calorimeter was intermittently heated, and surrounded by electrically heated and electronically controlled adiabatic shields. The substance was enclosed in an evacuated and sealed vitreous-silica tube of about 50 cm^3 volume, tightly fitted into the silver calorimeter. A central well in the tube served for the heater and platinum resistance thermometer.

The platinum resistance thermometer was calibrated locally at the ice, steam, zinc, and antimony points. Temperatures are judged to correspond to IPTS-68 within 0.05 K from 300 to 900 K and within 0.2 K at 1030 K. The accuracy in the energy inputs is about 0.03 per cent. The heat capacity of the empty calorimeter, including a vitreous-silica container, was determined in a separate series of experiments. The heat capacity of the 207.49 g sample represented about 52 per cent of the total. Corrections were applied for "zero drift" of the calorimeter and for differences in the masses of the silica containers.

875 *to* 1350 K, *enthalpy increments relative to* 298.15 K, *University of Oslo.* An aneroid drop calorimeter operating in air was used in the determinations. Details of the construction have been described[15] together with results obtained for a U.S. Fourth Calorimetry Conference sample of α-Al_2O_3.

About 5 g of FeAs was sealed in a vitreous-silica tube, which again was placed in a

TABLE 1. Molar heat capacity of iron monoarsenide ($R = 8.3144\ J \cdot K^{-1} \cdot mol^{-1}$; $M(FeAs) = 130.769\ g \cdot mol^{-1}$)

$\langle T \rangle$/K	$C_{p,m}/R$	$\langle T \rangle$/K	$C_{p,m}/R$	$\langle T \rangle$/K	$C_{p,m}/R$	$\langle T \rangle$/K	$C_{p,m}/R$	$\langle T \rangle$/K	$C_{p,m}/R$	$\langle T \rangle$/K	$C_{p,m}/R$
Low-temperature results—Ann Arbor											
Series I		221.97	5.64	76.85	2.541	73.96	2.425	75.07	2.464	Series X	
		232.16	5.71	78.72	2.625	74.22	2.432	75.63	2.488		
53.92	1.354	242.86	5.78					76.22	2.514	29.96	0.311
58.72	1.625	254.07	5.84	Series V		Series VI		76.81	2.539	32.64	0.396
63.82	1.935	265.17	5.91	65.87	2.069	$\Delta_{trs}H_m$ Detn. A		Series VIII		35.72	0.506
68.99	2.382	276.17	5.96	66.77	2.133	76.72	2.535			39.07	0.637
73.60	2.442	286.75	6.02	67.79	2.214			$\Delta_{trs}H_m$ Detn. B		42.76	0.795
77.99	2.592	296.91	6.07	68.50	2.280	Series VII		78.04	2.594	45.21	0.910
82.11	2.776	307.00	6.12	68.78	2.306	68.65	2.288				
85.98	2.948	316.34	6.17	69.06	2.338	68.92	2.318	Series IX		Series XI	
		324.93	6.21	69.33	2.369	69.18	2.351	4.85	0.003	47.52	1.018
Series II		333.47	6.24	69.60	2.408	69.44	2.382	5.60	0.005	51.65	1.230
84.49	2.882	342.84	6.28	69.86	2.452	69.70	2.425	6.88	0.006	56.64	1.503
89.36	3.087			70.12	2.505	69.95	2.469	8.39	0.009	61.60	1.794
96.47	3.354	Series IV		70.37	2.571	70.20	2.526	9.56	0.013	$\Delta_{trs}H_m$ Detn. C	
105.54	3.677	61.12	1.764	70.62	2.674	70.43	2.596	10.58	0.017	77.78	2.582
114.76	3.971	63.15	1.890	70.86	2.900	70.64	2.684	11.62	0.019		
124.27	4.240	64.59	1.983	71.10	2.740	70.85	2.889	12.79	0.025	Series XII	
134.30	4.488	65.51	2.043	71.34	2.535	71.05	2.818	14.00	0.031	70.32	2.549
144.89	4.704	66.44	2.107	71.60	2.464	71.27	2.569	15.29	0.040	70.44	2.578
		67.40	2.181	71.86	2.433	71.52	2.487	16.61	0.050	70.55	2.623
Series III		68.32	2.261	72.12	2.415	71.77	2.445	17.95	0.065	70.66	2.693
151.30	4.822	69.21	2.359	72.39	2.407	72.04	2.418	19.38	0.082	70.78	2.774
160.65	4.974	70.17	2.530	72.65	2.399	72.43	2.408	21.01	0.107	70.88	2.944
169.74	5.110	71.19	2.667	72.91	2.401	72.97	2.405	22.83	0.139	70.99	2.947
179.71	5.236	72.21	2.417	73.18	2.404	73.50	2.414	24.89	0.180	71.09	2.713
190.55	5.356	73.28	2.410	73.44	2.409	74.03	2.430	27.20	0.235	71.21	2.592
201.18	5.461	74.33	2.439	73.70	2.417	74.55	2.446	29.63	0.301	71.32	2.537
211.65	5.55	75.37	2.478								
High-temperature results—Oslo											
		390.62	6.38	502.65	6.76	663.94	7.30	774.74	7.69	909.56	8.15
Series XIII		400.78	6.43	512.90	6.80	673.08	7.29	787.49	7.69	922.65	8.16
309.03	6.06	410.94	6.46	523.16	6.85	676.32	7.38	800.36	7.72	935.76	8.26
319.28	6.12	421.10	6.49	539.92	6.88	685.67	7.33	813.26	7.79	948.88	8.32
329.49	6.16	431.27	6.54	556.72	6.91	698.34	7.29	826.12	7.87	962.02	8.41
339.69	6.20	446.54	6.61	602.70	7.07	711.07	7.40	838.90	7.97	975.18	8.47
349.89	6.24	461.81	6.70	613.88	7.11	723.79	7.43	851.69	8.00	988.35	8.53
360.09	6.29	471.98	6.67	626.97	7.19	736.54	7.48	864.60	8.00	1001.55	8.59
370.27	6.33	482.19	6.70	639.26	7.24	749.29	7.54	877.58	8.03	1014.78	8.64
380.45	6.35	492.41	6.74	651.56	7.27	762.04	7.61	890.59	8.09	1028.01	8.71

platinum and (platinum + 10 mass per cent of rhodium) container in a vertical tube furnace. The equilibrated sample assembly was hoisted into the silver calorimeter with electrically heated and electronically controlled adiabatic shields. The temperature increment of the calorimeter was measured with a quartz thermometer (Hewlett-Packard Model 2801A). The sample temperature in the furnace was measured with a Pt-to-(Pt + 10 per cent by mass of Rh) thermocouple. Uncertainty in the sample temperature, estimated to be about 1 K at 1350 K, represents the main source of error in the determinations.

3. Results and discussion

The experimental heat capacities for both the low- and high-temperature ranges are given in table 1. They are arranged in chronological order so that temperature increments used may in most cases be inferred from differences in successive mean temperatures.

LOW-TEMPERATURE HEAT CAPACITIES

A heat-capacity maximum is observed around 70 K (see figures 1 and 2). The transition was mapped with four series of determinations. Those of Series IV, V, and VII were made after the sample had been taken to 50 K only, while those of Series XII were made after cooling to 4 K. In these series different cooling rates and drift times were selected in order to reveal possible hysteresis in the transition. However, in all series the points nicely mapped a single peak with maximum at $T_N = (70.95 \pm 0.02)$ K. Three enthalpy-type determinations, A, B, and C in Series VI, VIII, and XI, were also made across the transition region (see table 2). The clearly cooperative part of the transition was estimated by bridging the region 60 to 77 K with heat capacities derived from a gradually changing Debye function with effective

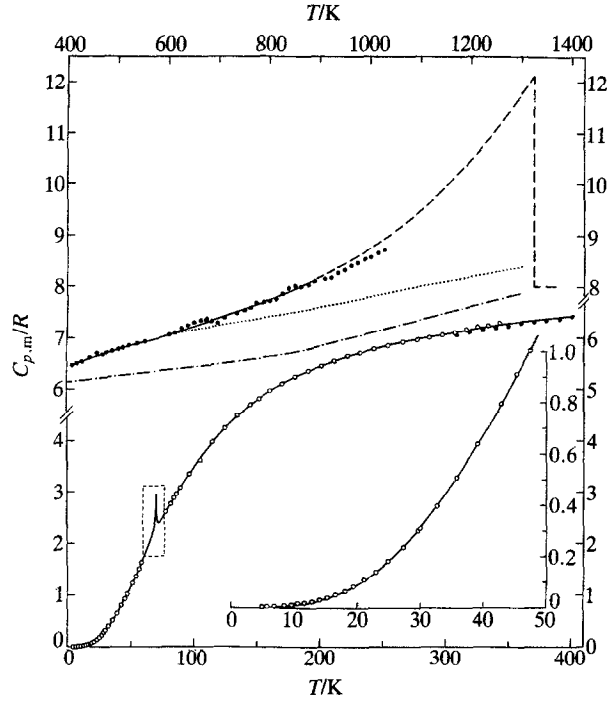

FIGURE 1. Heat capacity of FeAs. ○, Ann Arbor results; ●, Oslo results; — — —, estimated from drop calorimetry; —·—, estimated $C_{V,m}(l)+C_m(d)$; · · ·, estimated $C_{V,m}(l)+C_m(d)$ + C(Schottky) with E/hc and g: 0, 2; 300 cm^{-1}, 2; 1500 cm^{-1}, 2. For insert see figure 2.

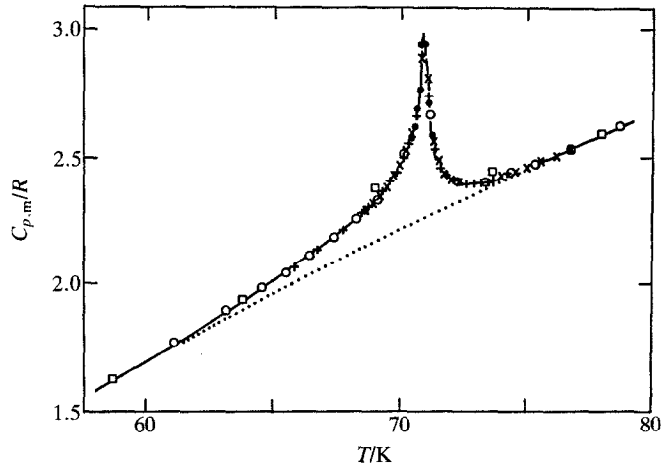

FIGURE 2. Low-temperature transition in FeAs. The different symbols represent different series (with various thermal histories) of determinations through the transitions region: □, Series I; ○, Series IV; +, Series V; ×, Series VII; ●, Series XII.

Θ_D values from 350.2 K at 50 K to 351.3 K at 90 K. The resulting transitional increments are

$$\Delta_{trs}H^\circ_m = 1.48R \cdot \mathrm{K} \quad \text{and} \quad \Delta_{trs}S^\circ_m = 0.021R.$$

In an earlier neutron-diffraction study[1] the transition temperature was found to be (77 ± 1) K and related to antiferromagnetic helical ordering of the iron atoms below this temperature. The integrated intensity of the magnetic satellites indicated $\boldsymbol{m} =$

TABLE 2. Molar enthalpy of transition determinations for iron monoarsenide
($R = 8.3144\ \mathrm{J \cdot K^{-1} \cdot mol^{-1}}$; $M(\mathrm{FeAs}) = 130.76\ \mathrm{g \cdot mol^{-1}}$)

Designation	$\frac{T_1}{\mathrm{K}}$	$\frac{T_2}{\mathrm{K}}$		$\frac{\Delta_{T_1}^{T_2}H^\circ_m}{R \cdot \mathrm{K}}$	$\frac{\Delta_{60\,\mathrm{K}}^{77\,\mathrm{K}}H^\circ_m}{R \cdot \mathrm{K}}$	$\frac{\Delta_{trs}H^\circ_m}{R \cdot \mathrm{K}}$
Detn. A.						
Series VI						
Meas. 1–2	62.959	64.707		3.379		
	64.710	75.484		25.262		
			$\Delta_{60\,\mathrm{K}}^{62.959\,\mathrm{K}}H^\circ_m$:	5.284		
			$\Delta_{75.484\,\mathrm{K}}^{77\,\mathrm{K}}$:	3.807	37.732	1.47
Detn. B						
Series VIII						
Meas. 1–2	62.951	64.572		3.126		
	64.575	76.671		28.504		
			$\Delta_{60\,\mathrm{K}}^{62.951\,\mathrm{K}}H^\circ_m$:	5.270		
			$\Delta_{76.671\,\mathrm{K}}^{77\,\mathrm{K}}H^\circ_m$:	0.836	37.736	1.48
Detn. C						
Series XI						
Meas. 5	63.991	76.389		28.933		
			$\Delta_{60\,\mathrm{K}}^{63.991\,\mathrm{K}}H^\circ_m$:	7.256		
			$\Delta_{76.389\,\mathrm{K}}^{77\,\mathrm{K}}H^\circ_m$:	1.550	37.739	1.48

$(0.5 \pm 0.1)\boldsymbol{m}_B$, where $\boldsymbol{m}_B$ denotes the Bohr magneton, which is only half of the magnetic moment expected for Fe(III) in the low-spin state.

The complexity of the helical pattern indicates the presence of various competing effects in the exchange interaction mechanisms. A careful analysis of possible direct and super-exchange paths suggests a minimum of seven different nearest-neighbor exchange constants. If isotropic exchange interaction is assumed and the classical Heisenberg energy used, the local stability conditions do determine both the ratio and the sign of two interaction parameters for a helical pattern.[16-20]

Moreover, by molecular-field theory, two relations $T_N = T_N\ (S, J_i/J_0;\ i = 1, \ldots, 6)$ and $\Theta_p = \Theta_p\ (S, J_i/J_0;\ i = 1, \ldots, 6)$, can be obtained,[18] where T_N is the Néel temperature, Θ_p the paramagnetic Curie temperature, S the spin, and J_i and J_0 the exchange interaction parameters involved. Therefore, with only three equations it is impossible to determine unambiguously the set of seven interaction constants. Further, the Θ_p relation cannot be used in this problem, due to the complicated behavior of the magnetic susceptibility. Even if the band structure were known, an unambiguous determination of the entire set of interaction constants would be impossible.

Finally, we remark on the striking difference of behavior between FeAs and CrAs.[2] The latter has nearly the same magnetic structure and distances as FeAs, but the transition takes place at $T_N = 259.9$ K and has considerable first-order character. It is, therefore, remarkable that in FeAs the magnetic transition is not coupled with a structural one.

HIGHER-TEMPERATURE HEAT CAPACITIES

The heat capacity of FeAs is increasingly high compared with classical behavior in the higher-temperature region. This is apparent from estimates of the constant-volume lattice heat capacity C_V(l), and the associated dilational heat capacity C(d) $= C_p - C_V$. For calculating C_V(l) in the higher-temperature region the Debye approximation was used with a single Debye temperature, taken as the maximum characteristic temperature ($\Theta_D = 353$ K at 90 K) in a plot against temperature after subtraction of estimated values of C(d) (see below).

According to Grüneisen:[21] $C_m(\mathrm{d}) = \alpha\Gamma C_{V,m}T$, where α is the isobaric expansivity and Γ is the Grüneisen parameter ($\alpha V_m/C_{V,m}\kappa$), where V_m is the molar volume and κ the isothermal compressibility. The isobaric expansivity of FeAs is known as a function of temperature from the X-ray work by Selte *et al.*[1] and $\kappa = 8.5 \times 10^{-12}$ Pa^{-1} at ambient temperature according, to Lyman and Prewitt.[11] Thus, $\Gamma = 2.27$, and the resulting constant-pressure lattice molar heat capacity is about 3 J·K^{-1}·mol^{-1} lower than that observed at 300 K and about 7 J·K^{-1}·mol^{-1} lower at 700 K. The discrepancy becomes increasingly larger with increasing temperature (see figure 1). An excess of this magnitude in the intermediate temperature range appears to be outside the influence of conduction-electron and anharmonic contributions to the heat capacity of FeAs. Thus, it is more probably caused by population of excited electronic states in iron, for which the magnetic moment and susceptibility behavior suggest a low-spin state.

For Fe^{3+} the six-fold degenerate $^2T_{2g}$ state is lowest in a regular octahedral ligand field. The orthorhombic deformation appears to result in a lower doublet, which is split under the influence of the exchange field in the low-temperature region. In consequence of this, the further contribution presumably arises from a 1:1:1 Schottky excitation. As can be seen from figure 1, the excess heat capacity in the intermediate region can be accounted for by the wavenumbers E/hc and degeneracies g: 0, 2; 1300 cm^{-1}, 2; 1500 cm^{-1}, 2.

Above 800 K the heat capacity shows considerably further increase, which will be considered after evaluation of the drop-calorimetric results.

DROP CALORIMETRY

The enthalpy-increment values relative to 298.15 K from drop calorimetry are given in table 3 for FeAs(cr) up to 1270 K, almost melted at 1324 K, and completely melted at 1354 K. The observed enthalpies up to 1270 were fitted to the polynomial: $\Delta^T_{298.15\,K}H^\circ_m/(R\cdot K) = a(T/K) + b(T/K)^2 + c(K/T) + d(T/K)^3 + e$, by least squares. The transition from adiabatic to drop-calorimetric results was smoothed by introducing enthalpy-increment values for 850, 900, 950, and 1000 K from adiabatic calorimetry with weight 6, and the restrictions $C_{p,m}$(FeAs, 800 K) = 7.75R and $\Delta^{800\,K}_{298.15\,K}H^\circ_m = 3467R\cdot K$. The resulting fit is shown in table 3. From 1323.9 to 1354.1 K the enthalpy increment corresponds to the average heat capacity $\langle C_{p,m}\rangle = 15.7R$, which indicates that melting is probably not complete at the former temperature. The melting temperature is taken as 1325 K, *i.e.* between the commonly reported value: 1303 K,[22-24] and that found by Selte *et al.*:[1] (1343 ± 20) K. By assuming the molar heat capacity of liquid FeAs to be 8.0R over the limited temperature in question and extrapolating the molar heat capacity of the solid to 12.1R at 1325 K, the molar enthalpy of fusion of FeAs is $\Delta_{fus}H^\circ_m = 6180R\cdot K$.

Entropies of fusion have been used to estimate the degree of ordering in solid and liquid intermetallic phases. If the solid intermetallic compound is completely ordered and the liquid disordered, entropies can be calculated from the entropies of fusion of the constituent elements by adding a disorder term $\Delta_{dis}S_m$. For a binary mixture this term is given by

$$\Delta_{dis}S_m = R(x_1 \ln x_1 + x_2 \ln x_2),$$

TABLE 3. Molar enthalpy-increment measurements—Oslo
($R = 8.3144\ J\cdot K^{-1}\cdot mol^{-1}$; M(FeAs) = 130.769 $g\cdot mol^{-1}$)

T/K	$\Delta^T_{298.15\,K}H^\circ_m/R\cdot K$ obs.	fit	T/K	$\Delta^T_{298.15\,K}H^\circ_m/R\cdot K$ obs.	fit	T/K	$\Delta^T_{298.15\,K}H^\circ_m/R\cdot K$ obs.	fit	T/K	$\Delta^T_{298.15\,K}H^\circ_m/R\cdot K$ obs.
874.1	4095	4053	1072.4	5773	5762	1172.3	6744	6731	1323.5	14432
874.1	4097	4053	1072.5	5778	5763	1269.0	7747	7768	1323.9	14545
970.0	4876	4850	1172.2	6744	6730	1270.5	7769	7785	1354.1	14833
970.0	4881	4850								

where x_1 and x_2 are the mole fractions of the two components. $\Delta_{dis}S_m = 1.386R$ for a compound of the type AB.

From the drop-calorimetric measurements the molar entropy of fusion of FeAs is $4.664R$ at 1325 K. The calculated molar entropy of fusion is $5.80R$, taking $\Delta_{fus}S^\circ_m(Fe) = 1.01R$,[25] and $\Delta_{fus}S^\circ_m(As) = 3.40R$.[26] This deviation indicates that some ordering is retained in the melt. The Fe atoms prefer As neighbors and *vice versa*. A complete analysis, however, is possible only within a series of isotypic compounds.

The high heat capacity of FeAs in the range 800 to 1325 K needs further consideration. A possible structural change from the MnP- to the NiAs-type presumably requires little energy and must, if present, occur just before melting. Thus, the excess heat capacity is more probably caused by the onset of a low- to high-spin transition of iron in the compound. Such a transition is accompanied by a large increase in volume and corresponding changes in the vibrational spectrum and entropy of the compound. It is not yet known if the driving force of this gradual transition stems from 3d electron redistribution only, structural defect formation, or other causes. In addition, some contribution from changing stoichiometry of the FeAs phase might be present at the highest temperatures.

It is a characteristic of the MnP- and NiAs-type structures that they possess interstitial positions capable of being occupied by metal atoms. Accordingly, a Frenkel-type disorder with equal numbers of normal and interstitial metal sites is possible. When the excess heat capacity of FeAs is analyzed by plotting $\lg\{\Delta_{exc}C_{p,m}T^2/(J\cdot K\cdot mol^{-1})\}$ against $1/T$ (see figure 3), an activation enthalpy of about $\Delta_{dis}H^\circ_m = 13000R\cdot K$ is found. The corresponding mole fraction of defects is about 0.065 at 1300 K. The values are reasonable, and the slight curvature in the plot might indicate small compositional changes at the higher temperatures. Further study of the underlying causes is needed.

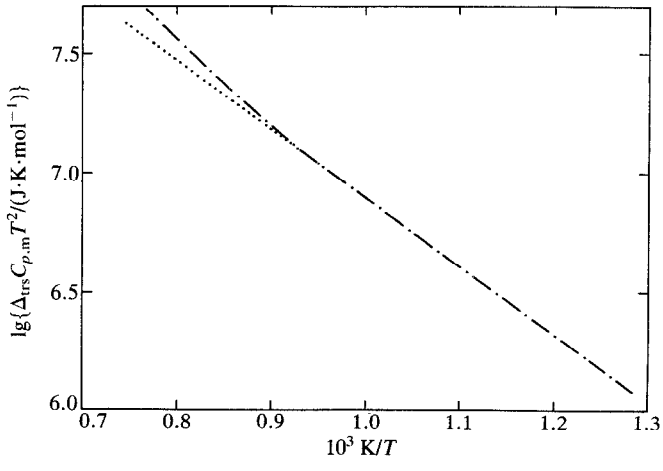

FIGURE 3. Plot for deriving enthalpy of defect formation in FeAs. — — —, Present results; ···, corresponds to $\Delta_{def}H^\circ_m \approx 13000R\cdot K$.

TABLE 4. Molar thermodynamic functions for iron monoarsenide FeAs
($R = 8.3144\ \mathrm{J \cdot K^{-1} \cdot mol^{-1}}$; $M(\mathrm{FeAs}) = 130.769\ \mathrm{g \cdot mol^{-1}}$)

$\frac{T}{\mathrm{K}}$	$\frac{C_{p,\mathrm{m}}}{R}$	$\frac{\Delta_0^T S_\mathrm{m}^\circ}{R}$	$\frac{\Delta_0^T H_\mathrm{m}^\circ}{R \cdot \mathrm{K}}$	$\frac{\Theta_\mathrm{m}^\circ}{R}$	$\frac{T}{\mathrm{K}}$	$\frac{C_{p,\mathrm{m}}}{R}$	$\frac{\Delta_0^T S_\mathrm{m}^\circ}{R}$	$\frac{\Delta_0^T H_\mathrm{m}^\circ}{R \cdot \mathrm{K}}$	$\frac{\Theta_\mathrm{m}^\circ}{R}$
5	0.004	0.003	0.005	0.002	240	5.773	6.229	832.1	2.762
10	0.014	0.008	0.045	0.003	250	5.831	6.465	890.1	2.905
15	0.038	0.018	0.168	0.007	260	5.885	6.695	948.7	3.046
20	0.091	0.035	0.472	0.011	270	5.934	6.918	1008	3.185
					273.15	5.950	6.987	1026	3.229
25	0.183	0.064	1.145	0.019					
30	0.313	0.109	2.35	0.030	280	5.980	7.134	1067	3.325
35	0.478	0.169	4.34	0.045	290	6.023	7.345	1127	3.458
40	0.676	0.245	7.19	0.065	298.15	6.057	7.513	1177	3.567
45	0.898	0.337	11.15	0.090	300	6.064	7.550	1188	3.591
					350	6.254	8.500	1496	4.226
50	1.144	0.445	16.21	0.120					
60	1.698	0.701	30.34	0.195	400	6.43	9.347	1813	4.814
70	2.479	1.011	50.68	0.287	450	6.60	10.12	2139	5.361
70.95[a]	(3.151)	1.017	54.56	0.288	500	6.77	10.82	2473	5.872
	[2.547][b]	[1.017]	[53.14]	[0.288]	550	6.92	11.47	2816	6.352
					600	7.07	12.08	3165	6.804
		λ-transition							
70.95[a]	(3.151)	1.038	56.05	0.288	650	7.22	12.65	3522	7.232
	[1.547]	[1.017]	[53.14]	[0.288]	700	7.39	13.19	3888	7.639
80	2.681	1.318	75.95	0.359	750	7.57	13.71	4262	8.026
					800	7.75	14.20	4644	8.398
90	3.106	1.684	105.04	0.517	850	7.97	14.68	5037	8.754
100	3.492	2.033	138.14	0.651					
110	3.823	2.381	174.8	0.792	900	8.20	15.14	5441	9.096
120	4.133	2.722	214.5	0.939	950	8.46	15.59	5857	9.426
130	4.369	3.066	256.9	1.090	1000	8.75	16.03	6287	9.745
					1050	9.10	16.47	6733	10.06
140	4.592	3.398	301.7	1.243	1100	9.49	16.90	7198	10.36
150	4.789	3.722	348.7	1.398	1150	9.95	17.33	7684	10.65
160	4.962	4.037	397.4	1.552	1200	10.48	17.77	8194	10.94
170	5.112	4.342	447.8	1.708	1250	11.07	18.21	8733	11.22
180	5.246	4.696	499.6	1.832	1300	(11.74)	18.65	9303	11.50
190	5.362	4.925	552.7	2.016	1325(s)	(12.09)	18.88	9600	11.63
200	5.465	5.203	606.8	2.169					
210	5.556	5.471	661.9	2.320	1325(l)	(8.0)	23.54	15780	11.63
220	5.636	5.732	717.9	2.470	1350	(8.0)	23.69	15980	11.85
230	5.708	5.984	774.7	2.616					

[a] Treating the 70.95 K λ-transition as though it were isothermal.
[b] Quantities in square brackets pertain to the lattice estimates.

THERMODYNAMIC FUNCTIONS

The experimental heat-capacity results were fitted to polynomials by the method of least squares, and integrated to yield values of thermodynamic functions at selected temperatures presented in table 4. Below 10 K the heat capacities were fitted and extrapolated linearly on a $C_{p,\mathrm{m}}/T$ against T^2 plot and the functions evaluated by extrapolation ($\gamma = 0.8 \times 10^{-3} R \cdot \mathrm{K}^{-1}$). Within the transition region the values were read from a large plot and the thermodynamic functions were calculated by

numerical integration of the curves with Simpson's rule. In the cryogenic region, the standard deviation of a single measured heat capacity is less than 1 per cent from 8 to 25 K, 0.1 per cent from 25 to 300 K, and 0.2 per cent from 300 to 350 K; in the superambient region, the estimated standard deviation in heat capacity is about 0.5 per cent up to 900 K. For the heat capacities derived from enthalpy increments it is about 3 per cent in the region 950 to 1270 K, and unknown at higher temperatures.

One of us (D.G.A.) gratefully acknowledges a grant from the Comite Conjunto Hispano Norteamericano para Asuntos Educativos y Culturales and another (G.K.) a grant from GRAFÖG (T.U. Clausthal). The authors thank Sven R. Svendsen for assistance in using his enthalpy-evaluation program.

REFERENCES

1. Selte, K.; Kjekshus, A.; Andresen, A. F. *Acta Chem. Scand.* **1972,** 26, 3101.
2. Blachnik, R.; Kudermann, G.; Grønvold, F.; Alles, A.; Falk, B.; Westrum, E. F., Jr. *J. Chem. Thermodynamics* **1978,** 10, 507.
3. Hägg, G. *Z. Krist.* **1928,** 68, 470.
4. Hägg, G. *Z. Krist.* **1929,** 71, 134.
5. Hägg, G. *Nova Acta Reg. Soc. Sci. Upsaliensis* **1929,** IV, 7, No. 1.
6. Fylking, K. E. *Arkiv Kemi Mineral. Geol.* **1934,** B11, No. 48.
7. Pfisterer, H.; Schubert, K. *Z. Metallk.* **1950,** 41, 358.
8. Selte, K.; Kjekshus, A. *Acta Chem. Scand.* **1969,** 23, 2047.
9. Selte, K. Thesis, University of Oslo, **1973.**
10. Selte, K.; Kjekshus, A. *Acta Chem. Scand.* **1973,** 27, 1448.
11. Lyman, P. S.; Prewitt, C. T. *Acta Cryst.* **1984,** B40, 14.
12. Hambling, P. G. *Acta Cryst.* **1953,** 6, 98.
13. Westrum, E. F., Jr.; Furukawa, G. T.; McCullough, J. P. *Experimental Thermodynamics.* Vol. 1. McCullough, J. P.; Scott, D. W.: editors. Butterworths: London. **1968,** p. 133.
14. Grønvold, F. *Acta Chem. Scand.* **1967,** 21, 1695.
15. Grønvold, F. *Acta Chem. Scand.* **1970,** 24, 1035.
16. Yoshimori, A. *J. Phys. Soc. Jpn* **1959,** 14, 807.
17. Takzuchi, S.; Motizuki, K. *Phys. Soc. Jpn* **1967,** 24, 742.
18. Nagamiya, T.; Nagata, K.; Kitano, Y. *Prog. Theor. Phys.* **1962,** 27, 1253.
19. Kitano, Y.; Nagamiya, T. *Prog. Theor. Phys.* **1964,** 31, 1.
20. Nagamiya, T. *Solid State Physics* **1967,** 20, 306.
21. Grüneisen, E. *Zustand des Festen Körpers, Handbuch der Physik X.* Springer: Berlin. **1926.**
22. Shunk, F. A. *Constitution of Binary Alloys.* Second Supplement. McGraw-Hill: New York. **1969.**
23. Kubaschewski, O. *Iron-Binary Phase Diagrams.* Springer: New York. **1982.**
24. Massalski, T. B.: editor-in-chief. *Binary Alloy Phase Diagrams.* Vol. 1. Am. Soc. Metals: Metals Park, Ohio. **1986.**
25. Hultgren, R.; Desai, P. D.; Hawkins, D.; Gleiser, M.; Kelly, K. K. *Selected Values of the Thermodynamic Properties of the Elements.* Am. Soc. Metals: Metals Park, Ohio. **1973.**
26. Baker, E. H. *Trans. Inst. Min. Metall. Sect. C* **1974,** 83, 237.